Applied Microbiology and Biotechnology (2019) 103:5215–5230
https://doi.org/10.1007/s00253-019-09815-x

BIOTECHNOLOGICAL PRODUCTS AND PROCESS ENGINEERING

Production of cellulosic butyrate and 3-hydroxybutyrate in engineered *Escherichia coli*

Dragan Miscevic[1] · Kajan Srirangan[2] · Teshager Kefale[1] · Daryoush Abedi[1,3] · Murray Moo-Young[1] · C. Perry Chou[1]

Received: 7 November 2018 / Revised: 20 March 2019 / Accepted: 31 March 2019 / Published online: 2 May 2019

Abstract

Being the most abundant renewable organic substance on Earth, lignocellulosic biomass has acted as an attractive and cost-effective feedstock for biobased production of value-added products. However, lignocellulosic biomass should be properly treated for its effective utilization during biotransformation. The current work aimed to demonstrate biobased production of butyrate and 3-hydroxybutyrate (3-HB) in engineered *Escherichia coli* using pretreated and detoxified aspen tree (*Populus tremuloides*) wood chips as the feedstock. Various bioprocessing and genetic/metabolic factors limiting the production of cellulosic butyrate and 3-HB were identified. With these developed bioprocessing strategies and strain engineering approaches, major carbons in the hydrolysate, including glucose, xylose, and even acetate, could be completely dissimilated during shake-flask cultivation with up to 1.68 g L^{-1} butyrate, 8.95 g L^{-1} 3-HB, and minimal side metabolites (i.e., acetate and ethanol) being obtained. Our results highlight the importance of consolidating bioprocess and genetic engineering strategies for effective biobased production from lignocellulosic biomass.

Keywords *Escherichia coli* · Lignocellulosic hydrolysate · Detoxification · Over-liming · Butyrate · 3-Hydroxybutyrate

Introduction

As a renewable feedstock and energy source, lignocellulosic materials are considered appealing for sustainable production of fuels and chemicals (Achinas and Euverink 2016; Delidovich et al. 2016; Jiang et al. 2017; Saini et al. 2015). In particular, the use of nonedible second-generation feedstocks, such as forest residues, perennial grasses, agricultural residues (e.g., corn stover), and municipal/industrial wastes, for biobased production can minimally affect food price (Balan 2014; Mohr and Raman 2013; Valentine et al. 2012).

Electronic supplementary material The online version of this article (https://doi.org/10.1007/s00253-019-09815-x) contains supplementary material, which is available to authorized users.

✉ C. Perry Chou
cpchou@uwaterloo.ca

[1] Department of Chemical Engineering, University of Waterloo, 200 University Avenue West, Waterloo, Ontario N2L 3G1, Canada

[2] Biotechnology Research Institute, National Research Council of Canada, Montreal, Quebec H4P 2R2, Canada

[3] Department of Drug & Food Control, Tehran University of Medical Sciences, Tehran, Iran

While lignocelluloses are abundant, their applications are often associated with high operating costs due to the requirement of pretreatment for releasing fermentable sugars (Brodeur et al. 2011; Carriquiry et al. 2011; Dionisi et al. 2015; Valdivia et al. 2016). On the other hand, the presence of various fermentation inhibitors in the pretreating stream can seriously affect the performance of subsequent cultivation (Jönsson et al. 2013). The formation of inhibitors is highly dependent on the types of feedstock and pretreatment technique. Common inhibitors found in the pretreating stream include aromatic compounds (e.g., phenols), furan aldehydes (e.g., furfural and 5-hydroxymethylfurfural), aliphatic carboxylates (e.g., acetate, formate, and levulinate), and inorganic compounds (e.g., $CaCl_2$ and NH_4Cl) (Cavka and Jönsson 2013; Fenske et al. 1998; J. Ulbricht et al. 1984; Jönsson et al. 2013). To counteract the inhibition issues, several detoxification strategies have been employed, including treatment with chemicals, enzymes, or microorganisms; heating and vaporization; and extraction (Alriksson et al. 2005a; Jönsson et al. 1998; Larsson et al. 1999; López et al. 2004; Persson et al. 2002b). Among various chemical detoxification methods, alkali treatment with $Ca(OH)_2$ or NH_4OH has been commonly used (Coz et al. 2016; Fakhrudin et al. 2014; Jönsson et al. 2013). In many cases, detoxification with

$Ca(OH)_2$ (i.e., over-liming) is regarded as an efficient and economical choice for inhibitor elimination (Larsson et al. 1999; Ranatunga et al. 2000). However, one drawback associated with over-liming detoxification is the excessive production of $CaSO_4$ and unwanted loss of fermentable sugars (Sateesh et al. 2011). Alternatively, detoxification using NH_4OH can result in lower sugar loss and more effective elimination of furfural inhibitors in comparison to the over-liming treatment (Alriksson et al. 2005a).

Here, we report biobased production of two short-chain fatty acids, i.e., butyrate and 3-hydroxybutyrate (3-HB), in engineered *Escherichia coli* using detoxified lignocellulosic hydrolysates as the feedstock. Short-chain fatty acids, such as acetate, propionate, and butyrate, are aliphatic monocarboxylates with wide-ranging industrial uses in food preparation, herbicide synthesis, and pharmaceutical applications (El-Shahawy Tarek Abd 2015; Entin-Meer et al. 2005; Wood 1998). Specifically, butyrate has been of particular interest for its potential pharmaceutical effects in treating leukemia, sickle cell anemia, and alopecia (Dwidar et al. 2012). Furthermore, 3-hydroxyalkanoates (or β-hydroxyalkanoates) are aliphatic carboxylates with a hydroxyl group attached to the β-carbon (Yu and Van Scott 2004). They are fine chemicals that can act as building blocks for the synthesis of several antibiotics, vitamins, and pheromones (Guevara-Martínez et al. 2015; Perez-Zabaleta et al. 2016; Ren et al. 2010). 3-HB is a common 3-hydroxyalkanoate that can also serve as a monomeric constituent of several biopolymers such as poly(3-hydroxybutyrate) (PHB) (Tokiwa and Ugwu 2007). Currently, butyrate and 3-HB are largely produced via chemical synthesis with various process limitations (Jawed et al. 2016; Welton 2015). Hence, there is a demand for biobased production of these two carboxylates using microbial platforms and cheap renewable feedstocks.

Biosynthesis of butyrate and 3-HB includes multiple and partially overlapped metabolic reactions with acetyl-CoA as the precursor, including (i) homo-fusion of two acetyl-CoA molecules to acetoacetyl-CoA, (ii) reduction of acetoacetyl-CoA to 3-hydroxybutyryl-CoA (3-HB-CoA), (iii) conversion of 3-HB-CoA to 3-HB directly or dehydration of 3-HB-CoA to crotonyl-CoA for subsequent butyrate production, (iv) conversion of crotonyl-CoA to butyryl-CoA, and (v) conversion of butyryl-CoA to butyrate (Fig. 1). Note that parallel routes via enantiomeric (*R*) and (*S*) forms of 3-HB-CoA exist in steps (ii) and (iii). Although microbial production of butyrate was previously demonstrated using native producers such as *Clostridium tyrobutyricum* and *Clostridium thermobutyricum* (Jha et al. 2014), the production was limited by numerous challenges, including strict anaerobic condition, narrow pH range, and low-level reducing equivalent (Baek et al. 2013). On the other hand, current biobased production of 3-HB can be laborious since it requires PHB biosynthesis in the native PHB-producer *Cupriavidus necator* followed by hydrolysis of PHB to 3-HB (Guevara-Martínez et al. 2015). Hence, genetic engineering of a robust host organism, such as *E. coli*, for biosynthesis of butyrate (Baek et al. 2013; Jawed et al. 2016) and 3-HB (Guevara-Martínez et al. 2015; Gulevich et al. 2017; Jarmander et al. 2015) has been explored. In this study, we first detoxified a pretreated lignocellulosic hydrolysate with alkali treatment. We then used the detoxified hydrolysate as the feedstock to cultivate selective engineered *E. coli* strains for butyrate and 3-HB production and to investigate various biosynthesis limitations. Subsequently, we identified several key genes for further genetic manipulation and strain engineering to enhance the production of cellulosic butyrate and 3-HB. With the developed biochemical and genetic engineering strategies, major carbons in the hydrolysate, including glucose, xylose, and even acetate, could be completely dissimilated during shake-flask cultivation with up to 1.68 g L^{-1} butyrate, 8.95 g L^{-1} 3-HB, and minimal side metabolites being obtained.

Materials and methods

Pretreatment and hydrolysis of lignocellulosic raw material

The lignocellulosic hydrolysate used in this study was derived from chipped wood of aspen tree (*Populus tremuloides*). The lignocellulosic raw material was thermochemically pretreated as described previously (Alriksson et al. 2011; Panagiotopoulos et al. 2013; Tian et al. 2017). Briefly, prior to steam pretreatment, 200 g of aspen wood chips was impregnated with a dilute H_2SO_4 solution (0.7 wt%) at room temperature overnight. The impregnated biomass was subsequently subjected to a steam treatment at 200 °C for 5 min. The resulting slurry was collected and then supplemented with cellulases and xylanases for incubation with shaking at 50 °C for 48 h. Following the hydrolysis, vacuum filtration was performed, and the pH of the filtered liquid fraction was adjusted to 2 with 12 M HCl solution to prevent microbial growth during storage. The hydrolysate was stored at 4 °C until further use.

Alkali treatments

Treatment of hydrolysate with $Ca(OH)_2$ was performed as described previously (Martinez et al. 2001). In brief, anhydrous $Ca(OH)_2$ (Alfa Aesar, MA, USA) was added to the lignocellulosic hydrolysate until pH 10 was reached. The mixture was first heated to 60 °C in a water bath for 30 min with vigorous mixing, then cooled to room temperature, and subsequently neutralized with 5 M H_2SO_4. On the other hand, treatment of hydrolysate with NH_4OH was carried out by adding 29% NH_4OH (Bio Basic, Inc., ON, Canada) until pH 10 was reached. The mixture was vigorously stirred at room

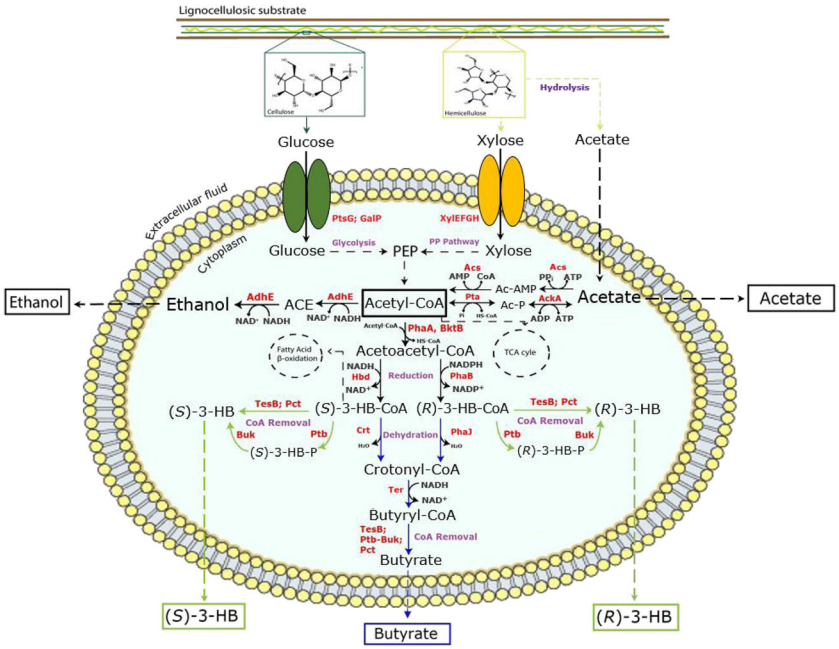

Fig. 1 Schematic representation of engineering key pathways in *E. coli* for heterologous production of butyrate and 3-HB from major carbons, including glucose, xylose, and acetate, in the lignocellulosic feedstock. Heterologous pathways outlined: butyrate pathway, in blue; 3-HB pathway, in green. Metabolic pathway abbreviations: PP pathway, pentose phosphate pathway; TCA cycle, tricarboxylic acid cycle. Metabolite abbreviations: Ac-P, acetyl phosphate; Ac-AMP, acetyladenylate; ACE, acetaldehyde; PEP, phosphoenolpyruvate; (*S*)/(*R*)-3-HB, (*S*)/(*R*)-3-hydroxybutyrate; (*S*)/(*R*)-3-HB-CoA, (*S*)/(*R*)-3-hydroxybutyryl-CoA; (*S*)/(*R*)-3-HB-P, (*S*)/(*R*)-3-hydroxybutyryl phosphate; (*S*)/(*R*)-butyryl-P, (*S*)/(*R*)-butyryl phosphate. Protein abbreviations: AckA, acetate kinase; Acs, acetyl-CoA synthetase; AdhE, aldehyde-alcohol dehydrogenase; BktB, β-ketothiolase; Buk, butyrate kinase; Crt, crotonase; GalP, galactose permease; Hbd, (*S*)-3HB-CoA dehydrogenase; Pct, acetate/propionate CoA-transferase; PhaA; acetoacetyl-CoA thiolase; PhaB, (*R*)-3HB-CoA dehydrogenase; PhaJ, (*R*)-specific enoyl-CoA hydratase; Pta, phosphotransacetylase; Ptb, phosphate butyryltransferase; PtsG, PTS system glucose-specific EIICB component; Ter, *trans*-2-enoyl-CoA reductase; TesB, Acyl-CoA thioesterase II; XylEFGH, D-xylose transporter

temperature for 30 min, pH-adjusted to 7 with 5 M H_2SO_4, and then centrifuged at 8,000×*g* for 5 min (Alriksson et al. 2005a). The supernatant was collected and filtered using a membrane with 0.45 μm pore size.

Bacterial strains and plasmids

Bacterial strains and plasmids used in this study are listed in Table 1, and DNA primers are listed in Table S1. Genomic DNA from bacterial cells was isolated using the Blood & Tissue DNA Isolation Kit (Qiagen, Hilden, Germany). Standard recombinant DNA technologies were applied for molecular cloning (Miller 1992). All plasmids were constructed by Gibson enzymatic assembly (Gibson et al. 2009). Phusion HF and *Taq* DNA polymerases were obtained from New England Biolabs (Ipswich, MA, USA). All synthesized oligonucleotides were obtained from Integrated DNA Technologies (Coralville, IA, USA). DNA sequencing was conducted by the Centre for Applied Genomics at the Hospital for Sick Children (Toronto, Canada). *E. coli* BW25113 was the parental strain for derivation of all mutant strains in this study, and *E. coli* DH5α was used as a host for molecular cloning.

Selective gene knockouts were introduced into BWΔ*ldhA* by P1 phage transduction (Miller 1992) using the appropriate Keio Collection strains (The Coli Genetic Stock Center, Yale University, New Haven, CT, USA) as donors (Baba et al. 2006). To eliminate the co-transduced FRT-Kn^R-FRT cassette, the transductants were transformed with pCP20 (Cherepanov and Wackernagel 1995), a temperature-sensitive plasmid expressing a FLP-recombinase. Upon Flp-mediated excision of the Kn^R cassette, a single Flp recognition site (FRT "scar site") was generated. Plasmid pCP20 was then cured by growing cells at 42 °C. The genotypes of derived knockout strains were confirmed by colony PCR using the appropriate verification primer sets listed in Table S1.

Plasmid pTrc-PhaAB-Crt-Ter was constructed by PCR-amplifying *phaAB* operon (accession number: J04987), *crt* (accession number: U17110), and *ter* (accession number: AE017226) from the genomic DNA of *C. necator* ATCC 43291, *Clostridium acetobutylicum* ATCC 824, and *Treponema denticola* ATCC 35405, respectively, using the corresponding primer sets (i.e., g-phaAB, g-crt, and g-ter), and all three fragments were Gibson-assembled (note that "assembled" is used for subsequent appearance) with the PCR-linearized pTrc99a vector using the primer set g-pTrc-phaAB-crt-ter. Expression of the genes inserted into pTrc99a

Table 1 *E. coli* strains and plasmids used in this study

Strain or plasmid	Description and relevant genotype	Source
E. coli host strains		
DH5α	F-, *endA1*, *glnV44*, *thi-1*, *recA1*, *relA1*, *gyrA96*, *deoR*, *nupG φ80d lacZΔ M15*, Δ(*lacZYA – argF*) *U169*, *hsdR17* (*rK-mK +*), λ-	Lab stock
BW25141	F-, Δ(*araD-araB*)*567*, Δ*lacZ4787* (::*rrnB-3*), Δ(*phoB-phoR*)*580*, λ-, *galU95*, Δ*uidA3*::*pir +*, *recA1*, *endA9* (*del-ins*)::*FRT*, *rph-1*, Δ(*rhaD-rhaB*)*568*, *hsdR514*	(Datsenko and Wanner 2000)
BW25113	F-, Δ(*araD-araB*)*567*, Δ*lacZ4787*(::*rrnB-3*), λ-, *rph-1*, Δ(*rhaD-rhaB*)*568*, *hsdR514*	(Datsenko and Wanner 2000)
BWΔldhA	BW25113 ldhA null mutant	(Akawi et al. 2015)
PC-C4A0	BWΔldhA/pTrc-PhaAB-Crt-Ter and pK-BktB-Hbd	This study
PC-C4A1	BWΔldhA/pTrc-PhaAB-Crt-Ter and pK-BktB-Hbd-TesB	This study
PC-C4A2	BWΔldhA/pTrc-PhaAB-Crt-Ter and pK-BktB-Hbd-Ptb-Buk	This study
PC-C4A3	BWΔldhA/pTrc-PhaAB-Crt-Ter and pK-BktB-Hbd-Pct	This study
PC-3HBR	BWΔldhA/pTrc-PhaAB and pK-BktB-TesB	This study
PC-3HBS	BWΔldhA/pTrc-PhaA and pK-BktB-Hbd-TesB	This study
PC-3HBRS	BWΔldhA/pTrc-PhaAB and pK-BktB-Hbd-TesB	This study
PC-3HBRSΔ*arcA*	*arcA* null mutant of PC-3HBRS	This study
PC-3HBRSΔ*fnr*	*fnr* null mutant of PC-3HBRS	This study
PC-BA0	BWΔldhA/pTrc-PhaA-Ter and pK-BktB-Ptb-Buk	This study
PC-BAR	BWΔldhA/pTrc-PhaAB-Ter and pK-BktB-PhaJ-Ptb-Buk	This study
PC-BAS	BWΔldhA/pTrc-PhaA-Crt-Ter and pK-BktB-Hbd-Ptb-Buk	This study
PC-BARS	BWΔldhA/pTrc-PhaAB-Crt-Ter and pK-BktB-Hbd-PhaJ-Ptb-Buk	This study
Plasmids		
pTrc99a	ColE1 ori Apr P*trc*	(Amann et al. 1988)
pK184	p15A ori, KmR, P*lac::lacZ*'	(Jobling and Holmes 1990)
pTrc-PhaA-Ter	Derived from pTrc99a, P_{trc}::*phaA:ter*	This study
pTrc-PhaAB-Crt-Ter	Derived from pTrc99a, P_{trc}::*phaAB:crt:ter*	This study
pTrc-PhaAB-Ter	Derived from pTrc99a, P_{trc}::*phaAB:ter*	This study
pTrc-PhaA-Crt-Ter	Derived from pTrc99a, P_{trc}::*phaA:crt:ter*	This study
pTrc-PhaA	Derived from pTrc99a, P_{trc}::*phaA*	This study
pTrc-PhaAB	Derived from pTrc99a, P_{trc}::*phaAB*	This study
pK-BktB-Hbd-TesB	Derived from pK184, P_{lac}::*bktB:hbd:tesB*	This study
pK-BktB-Hbd-Ptb-Buk	Derived from pK184, P_{lac}::*bktB:hbd:ptb:buk*	This study
pK-BktB-Hbd-Pct	Derived from pK184, P_{lac}::*bktB:hbd:pct*	This study
pK-BktB-Hbd	Derived from pK184, P_{lac}::*bktB:hbd*	This study
pK-BktB-PhaJ-Ptb-Buk	Derived from pK184, P_{lac}::*bktB:phaJ:ptb:buk*	This study
pK-BktB-Ptb-Buk	Derived from pK184, P_{lac}::*bktB:ptb:buk*	This study
pK-BktB-Hbd-PhaJ-Ptb-Buk	Derived from pK184, P_{lac}::*bktB:hbd:phaJ:ptb:buk*	This study

vector was under the control of the P_{trc} promoter. The *phaAB* operon was amplified by using the primer set g-phaAB2 from pTrc-PhaAB-Crt-Ter plasmid, and the amplicon was subsequently assembled with PCR-linearized pTrc99a using the primer set g-pTrc-phaAB, generating pTrc-PhaAB. The DNA fragment *phaA* from pTrc-PhaAB was PCR-amplified using the primer set g-phaA, and then assembled with the PCR-linearized pTrc99a using the corresponding primer set g-pTrc-phaA, generating pTrc-PhaA. The *phaA* and *ter* genes were individually PCR-amplified from pTrc-PhaAB-Crt-Ter using the primer sets of g-phaA and g-ter2, respectively, and the two amplicons were assembled with PCR-linearized pTrc99a using the primer set g-pTrc-phaA-ter to generate pTrc-PhaA-Ter. To construct pTrc-PhaAB-Ter, the *phaAB* operon and *ter* gene were individually PCR-amplified from pTrc-PhaAB-Crt-Ter plasmid using the primer sets g-phaAB3 and g-ter3, respectively. The amplicon was then assembled with the PCR-linearized pTrc99a using the primer set g-pTrc-phaAB-ter. To generate pTrc-PhaA-Crt-Ter, the *crt* gene was PCR-amplified from pTrc-PhaAB-Crt-Ter using the primer set g-crt2, and the

amplicon was assembled with PCR-linearized pTrc-PhaA-Ter using the primer set g-pTrc-phaA-crt-ter. Plasmid pK-BktB-Hbd-TesB was constructed by PCR-amplifying *bktB* (accession number: AF026544), *hbd* (accession number: U17110), and *tesB* (accession number: M63308) from the genomic DNA of *C. necator* ATCC 43291, *C. acetobutylicum* ATCC 824, and *E. coli* BW 25141, respectively, using the corresponding primer sets (i.e., g-bktB, g-hbd, and g-tesB), followed by assembling the three amplicons with the PCR-linearized pK184 using the primer set g-pK-bktB-hbd-tesB. Expression of the genes inserted into pK184 was under the control of the P_{lac} promoter. Plasmid pK-BktB-Hbd was constructed by PCR-amplifying *hbd* from pK184-BktB-Hbd-TesB using the primer set g-pK-bktB-hbd, followed by assembling the amplicon with the PCR-linearized pK-BktB using the primer set g-pK-bktB. To generate pK-BktB-Hbd-Ptb-Buk and pK-BktB-Hbd-Pct, the *ptb-buk* operon (accession number: AE001437) from the genomic DNA of *C. acetobutylicum* ATCC 824 and *pct* (accession number: AJ276553) from the genomic DNA of *Clostridium propionicum* DSM 1682 were PCR-amplified using the corresponding primer sets of g-ptb-buk and g-pct, respectively. The *ptb-buk* and *pct* amplicons were then individually assembled with PCR-linearized pK-BktB-Hbd using the g-pK-bktB-hbd-ptb-buk and g-pK-bktB-hbd-pct primer sets, respectively. The *bktB* gene and *ptb-buk* operon were individually PCR-amplified from pK-BktB-Hbd-Ptb-Buk using the g-bktB2 and g-ptb-buk2 primer sets, respectively. The two amplicons were assembled with PCR-linearized pK184 using the primer set g-pK-bktB-ptb-buk to generate pK-BktB-Ptb-Buk. To generate pK-BktB-PhaJ-Ptb-Buk, *phaJ* (accession number: BAA21816) was PCR-amplified from the genomic DNA of *Aeromonas caviae* ATCC 15468 using the g-phaJ primer set. The amplicon was assembled with PCR-linearized pK-BktB-Ptb-Buk using the g-pK-bktB-phaJ-ptb-buk primer set. Lastly, pK-BktB-Hbd-PhaJ-Ptb-Buk was generated by PCR-amplifying the *hbd* gene from pK-BktB-Hbd-TesB using the primer set g-hbd2, followed by assembling the amplicon with PCR-linearized pK-BktB-PhaJ-Ptb-Buk using the primer set g-pK-bktB-hbd-phaJ-ptb-buk.

Media and cultivations

All medium components were obtained from Sigma-Aldrich Co. (St Louis, MO, USA) except glucose, yeast extract, and tryptone which were obtained from BD Diagnostic Systems (Franklin Lakes, NJ, USA). The media were supplemented with antibiotics as required: 25 μg mL^{-1} kanamycin and 50 μg mL^{-1} ampicillin. For cell revival, *E. coli* strains, stored as glycerol stocks at − 80 °C, were streaked on LB agar plates with appropriate antibiotics and incubated at 37 °C for 14–16 h. Single colonies were picked from the LB plates to inoculate 30 mL LB medium (10 g L^{-1} tryptone, 5 g L^{-1} yeast extract, and 5 g L^{-1} NaCl) with appropriate antibiotics in 125-mL conical flasks. The cultures were shaken at 37 °C and 280 rpm in a rotary shaker (New Brunswick Scientific, NJ, USA) and used as seed cultures to inoculate 220 mL LB media at 1% (*v*/*v*) with appropriate antibiotics in 1-L conical flasks. This second seed culture was shaken at 37 °C and 280 rpm until an optical density of 0.8 OD_{600} was reached. Cells were then harvested by centrifugation at 9,000×*g* and 20 °C for 10 min and resuspended in 30 mL modified M9 production media. The suspended culture was transferred into 125-mL screw cap plastic production flasks and incubated at either 30 or 37 °C at 280 rpm in a rotary shaker for 48 h. Note that the termination period for all cultivations was selected in accordance with our previous time-point experimentations demonstrating maximal 3-HB and butyrate titers to be around 48 h (data not shown). Unless otherwise specified, the modified M9 production medium contained 58% (*v*/*v*) hydrolysate, 5 g L^{-1} yeast extract, 10 mM $NaHCO_3$, 1 mM $MgCl_2$, 200 mL L^{-1} of M9 salts mix (33.9 g L^{-1} Na_2HPO_4, 15 g L^{-1} KH_2PO_4, 5 g L^{-1} NH_4Cl, 2.5 g L^{-1} NaCl), 1 mL L^{-1} of Trace Metal Mix A5 (2.86 g L^{-1} H_3BO_3, 1.81 g L^{-1} $MnCl_2•4H_2O$, 0.22 g L^{-1} $ZnSO_4•7H_2O$, 0.39 g L^{-1} $Na_2MoO_4•2H_2O$, 79 μg L^{-1} $CuSO_4•5H_2O$, and 49.4 μg L^{-1} $Co(NO_3)_2•6H_2O$), and supplemented with 0.10 mM isopropyl β-D-1-thiogalactopyranoside (IPTG). All cultivation experiments were performed in triplicate.

Analytical procedures

Culture samples were appropriately diluted with 0.15 M saline solution for measuring cell density in OD_{600} using a spectrophotometer (DU520, Beckman Coulter, Fullerton, CA). For high-performance liquid chromatography (HPLC) and nuclear magnetic resonance (NMR) analysis, cell-free medium was collected by centrifugation of the culture sample at 9,000×*g* for 5 min followed by filter sterilization using a 0.2-μM syringe filter.

HPLC analysis

Extracellular metabolites, i.e., organic acids and sugars, were quantified using HPLC (LC-10AT, Shimadzu, Kyoto, Japan) with a refractive index detector (RID; RID-10A, Shimadzu, Kyoto, Japan) and a chromatographic column (Aminex HPX-87H, Bio-Rad Laboratories, CA, USA). The HPLC column temperature was maintained at 65 °C, and the mobile phase was 5 mM H_2SO_4 (pH 2) running at 0.6 mL min^{-1}. The RID signal was acquired and processed by a data processing unit (Clarity Lite, DataApex, Prague, Czech Republic).

NMR analysis

Extracellular medium samples were diluted in 10% (*v*/*v*) with an internal standard solution composed of 99.9% D_2O with 5 mM 2,2-dimethyl-2-silapentane-5-sulfonate (DSS) as a chemical shape indicator (CSI) and 0.2% (*w*/*v*) sodium azide

(NaN_3) for the inhibition of bacterial growth. The diluted samples were subsequently transferred to 5-mm NMR tubes (NE-UL5-7, New Era Enterprises Inc., Vineland, NJ). Spectra were acquired by a one-dimensional Nuclear Overhauser Effect Spectroscopy (1D NOESY) pulse sequence on a Bruker Avance 600.13 MHz spectrometer with a TXI 600 Probe (Bruker Canada Ltd., Toronto, Canada). Following data acquisition, the spectra were imported to Chenomx NMR Suite 7.5 (Chenomx Inc., Edmonton, Alberta, Canada) for data processing with phase, baseline, shim, and shape corrections being carried out. An average sample pH of 5.2 measured during fermentation was applied as a reference for metabolite identification. Following spectral processing, various extracellular metabolites were identified by targeted profiling.

Results

Butyrate and 3-HB biosynthesis in engineered *E. coli*

For biosynthesis of butyrate and 3-HB, a double plasmid system was employed in *E. coli* PC-C4A1 (Fig. 2) to implement key metabolic pathways (Fig. 1). First, homo-fusion of two acetyl-CoA moieties into acetoacetyl-CoA was carried out by two β-ketothiolases, i.e., PhaA and BktB. Subsequently, acetoacetyl-CoA is reduced to (*S*)-3-hydroxybutyryl-CoA (3-HB-CoA) by NADH-dependent Hbd or (*R*)-3-HB-CoA by NADPH-dependent PhaB. Both (*R*)-3-HB-CoA and (*S*)-3-HB-CoA can be converted to (*R*)-3-HB and (*S*)-3-HB, respectively, by a CoA-removing enzyme, such as Pct, TesB, or Ptb/Buk. Alternatively, (*R*)-3-HB-CoA and (*S*)-3-HB-CoA can be converted to crotonyl-CoA by PhaJ and Crt, respectively. Crotonyl-CoA is then reduced to butyryl-CoA by NADH-dependent Ter, and subsequently converted to butyrate by one of the above CoA-removing enzymes.

Using the NMR analysis, the original (undetoxified and undiluted) hydrolysate used in this study was determined to contain approximately 65 g L^{-1} glucose, 28 g L^{-1} xylose, 12 g L^{-1} acetate, and trace amounts of inhibitors, i.e., furan derivatives, phenolic compounds, and benzoates. Note that after mixing with the cultivation base medium, the initial concentrations decreased to 41 g L^{-1} glucose, 17 g L^{-1} xylose, and 8 g L^{-1} acetate. PC-C4A1 was cultivated in a shake-flask at 37 °C using the original hydrolysate as the feedstock (Fig. 2b), producing 1.04 g L^{-1} butyrate and 1.72 g L^{-1} 3-HB. In addition to 8 g L^{-1} acetate already residing in the original hydrolysate, the PC-C4A1 cultivation produced 4 g L^{-1} acetate and 0.55 g L^{-1} ethanol. To evaluate the effects of the inhibitors in the original hydrolysate, we cultivated PC-C4A1 at 37 °C in a shake-flask using a defined medium containing 39 g L^{-1} glucose, 15 g L^{-1} xylose, and 8 g L^{-1} acetate (Fig. 2a). Sugar consumption for the two cultures was rather similar. Compared to the culture using the original hydrolysate, the culture using the defined medium had a similar level of 3-HB production but significantly lower butyrate production. Note that ethanol production was 6-fold higher with no extra acetate formation in the defined medium, contrary to the results using the original hydrolysate, suggesting a potential redirection of carbon flux at the acetyl-CoA node from ethanologenesis to acetogenesis when consuming the original hydrolysate.

Chemical detoxification of hydrolysate

In an attempt to reduce toxic components in the original hydrolysate for enhanced butyrate and 3-HB production, two chemical detoxification methods were performed, i.e., (i) $Ca(OH)_2$ treatment (i.e., over-liming) and (ii) NH_4OH treatment. To evaluate the detoxification efficiency, PC-C4A1 was cultivated in a 37 °C shake-flask using the detoxified hydrolysates (Fig. 2c, d). Following the over-liming detoxification by adding 2.4% (*w*/*v*) $Ca(OH)_2$ to the original hydrolysate as previously suggested (Martinez et al. 2000; Martinez et al. 2001; Okuda et al. 2008), the concentrations of glucose and xylose were reduced by 22% and 9%, respectively, whereas the acetate concentration remained unchanged, in comparison to the original hydrolysate. However, these carbons, even including acetate, in the $Ca(OH)_2$-detoxified hydrolysate were effectively dissimilated during the cultivation, resulting in significantly higher cell density (40% higher) and 3-HB concentration (180% higher) than those of the cultivation using the original hydrolysate. Our previous time-point experimentations also show complete sugar and acetate dissimilation by 48-h period (data not shown). Also, note that butyrate production was slightly reduced in the culture using the $Ca(OH)_2$-detoxified hydrolysate. On the other hand, the glucose and xylose concentrations were slightly reduced (5% and 6.5%, respectively) with a relatively unchanged acetate concentration upon the NH_4OH treatment by adding 29% NH_4OH to the original hydrolysate as described previously (Alriksson et al. 2005b). Although the loss of fermentable sugars was lower for the NH_4OH-treated hydrolysate in comparison to the $Ca(OH)_2$-treated hydrolysate, the NH_4OH treatment did not result in any improvement in producing 3-HB or butyrate. Note that, similar to the control cultivation using the original hydrolysate, dissimilation of glucose and xylose was rather incomplete, and there was an extra acetate accumulation during the cultivation with the NH_4OH-treated hydrolysate. These results suggest that the $Ca(OH)_2$ treatment could significantly reduce the toxicity in the original hydrolysate for the enhanced production of 3-HB and butyrate. Hence, the $Ca(OH)_2$-detoxified hydrolysate was used for all subsequent cultivation experiments.

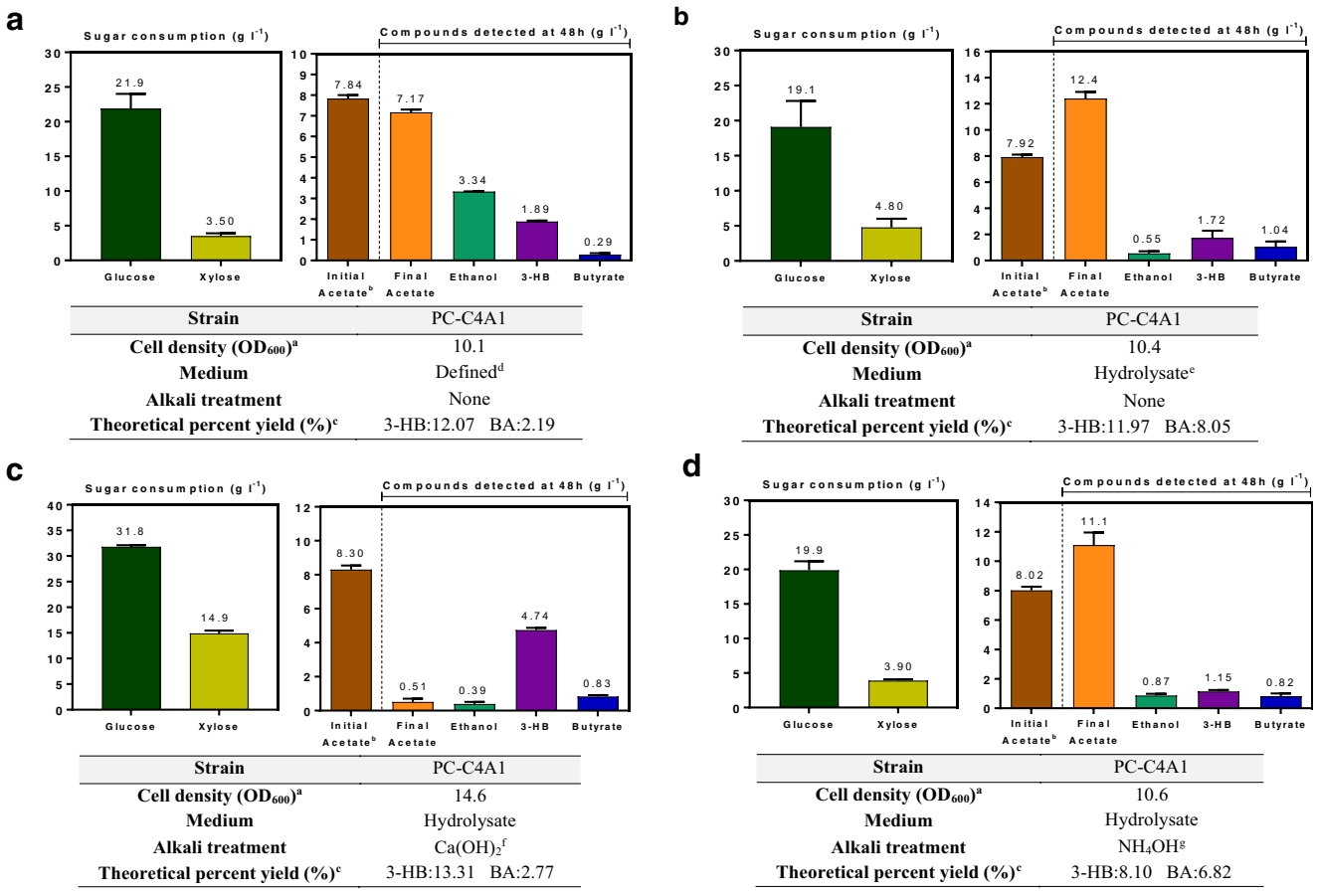

[a] Measured cell density after 48 h cultivation using spectrophotometer (OD_{600}), time 0h cell density was kept at ~5.00
[b] Acetate concentration (g l^{-1}) at 0h
[c] Defined as the percentage of 3-HB/butyrate theoretical yields based on consumed glucose, xylose, and acetate
[d] Defined medium mixture containing 39.0±0.1 g l^{-1} glucose, 15.2±0.2 g l^{-1} xylose, and 7.84±0.2 g l^{-1} acetate
[e] Original hydrolysate feedstock; initial glucose, xylose, and acetate concentrations of 41.2±0.7 g l^{-1}, 17.0±0.3 g l^{-1}, and 7.9±0.2 g l^{-1}, respectively
[f] 2.4% (w/v) $Ca(OH)_2$ detoxification at 60°C for 30 minutes; after treatment initial glucose, xylose, and acetate concentrations were 32.1±0.8 g l^{-1}, 15.4±0.7 g l^{-1}, and 8.3±0.4 g l^{-1}, respectively
[g] 25% (w/v) NH_4OH detoxification at RT for 30 minutes; after treatment initial glucose, xylose, and acetate concentrations were 39.0±1.2 g l^{-1}, 15.9±0.9 g l^{-1}, and 8.0±0.2g l^{-1}, respectively
BA butyrate

Fig. 2 Metabolic profile of PC-C4A1 using defined and hydrolysate-treated culture media under 37 °C cultivation temperature. Sugar consumption, major metabolite titers, and final optical density during cultivation of PC-C4A exposed to defined medium (**a**), original hydrolysate (**b**), $Ca(OH)_2$-treated hydrolysate (**c**), and NH_4OH-treated hydrolysate (**d**). Error bars represent the mean ± SD (n = 3)

Manipulation of CoA-removing mechanism

For enhanced acid production, we also engineered the production strains by genetic manipulation of various enzymes involved in the biosynthesis of 3-HB and butyrate. It has been our recent observation that the CoA-removing step often represents a key step limiting the overall acid production (data not published). In addition to the native TesB, two other CoA-removing enzymes were evaluated here, i.e., Ptb-Buk from *C. acetobutylicum* ATCC 824 and Pct from *C. propionicum* DSM 1682. Given that both Ptb-Buk and Pct originate from organisms with an optimal metabolic activity at temperatures different from those of *E. coli*, we examined the effects of CoA-removing enzymes at two temperatures of 30 °C (Fig. 3) and 37 °C (Fig. 4). Under both 30 °C and 37 °C, the control strain PC-C4A0 lacking a gene encoding a CoA-removing enzyme did not generate any 3-HB. While PC-C4A0 did not produce any butyrate at 30 °C, it produced a low level of butyrate at 0.04 g L^{-1} at 37 °C, presumably due to the activity of the native phosphotransacetylase-acetate kinase (Pta-AckA) and/or other putative thioesterases (Volker et al. 2014). Notably, it appears that the consumption of glucose, xylose, and acetate was more effective under the low temperature of 30 °C. However, such effective carbon consumption did not necessarily result in better acid production. For PC-C4A1, which episomally expressed *tesB*, 3-HB production was slightly favored at a higher temperature, i.e., 4.48 g L^{-1} at 30 °C (Fig. 3b) vs. 4.74 g L^{-1} at 37 °C (Fig. 2c), while butyrate production was similar for both cultivation temperatures. In contrast, PC-C4A2 expressing the *ptb-buk* operon produced more 3-HB under a lower temperature, i.e., 1.07 g L^{-1} at 30 °C and 0.52 g L^{-1} at 37 °C, but produced more butyrate at a higher temperature, i.e., 1.03 g L^{-1} at 30 °C and 1.20 g L^{-1} at 37 °C. Expression of *pct* in PC-C4A3 resulted in comparable 3-HB titers for the two cultivation temperatures

and slightly higher butyrate production at a lower temperature, i.e., 0.84 g L^{-1} at 30 °C and 0.67 g L^{-1} at 37 °C. Generally, the two strains with high 3-HB and butyrate production, i.e., PC-C4A1 and PC-C4A2, respectively, were cultivated under 37 °C. The biosynthesis of 3-HB by PC-C4A1 at 37 °C (Fig. 2c) was approximately 9-fold and 5.5-fold that of PC-C4A2 (Fig. 4b) and PC-C4A3 (Fig. 4c), respectively, suggesting that TesB was the most effective enzyme for the conversion of (*S*)/(*R*)-3-HB-CoA to (*S*)/(*R*)-3-HB. On the other hand, the biosynthesis of butyrate by PC-C4A2 at 37 °C was approximately 1.5-fold and 1.8-fold that of PC-C4A1 and PC-C4A3, respectively, suggesting that Ptb-Buk was the most effective enzyme system for the conversion of butyryl-CoA to butyrate. Hence, TesB and Ptb-Buk were chosen as the CoA-removing enzymes for subsequent strain engineering for enhanced production of 3-HB and butyrate, respectively.

Manipulation of the butyrate-producing pathway

There are two parallel reduction-dehydration (RD) routes leading to butyrate biosynthesis (Fig. 1), i.e., the Hbd-Crt and PhaB-PhaJ branches which drive the conversion from acetoacetyl-CoA to crotonyl-CoA via (*S*)-3-HB-CoA and (*R*)-3-HB-CoA, respectively. The engineered strains discussed thus far contain only the Hbd-Crt branch. To increase the intracellular crotonyl-CoA pool, we further introduced the PhaB-PhaJ branch by expressing *phaJ* encoding enoyl-CoA hydratase from *A. caviae* (Bond-Watts et al. 2011; Lan and Liao 2012). Butyrate production based on individual and both RD routes in various engineered strains is summarized in Fig. 5. The control strain PC-BA0 lacking both RD routes produced neither butyrate nor 3-HB. The biosynthesis of butyrate via the Hbd-Crt route in PC-BAS was 2.4-

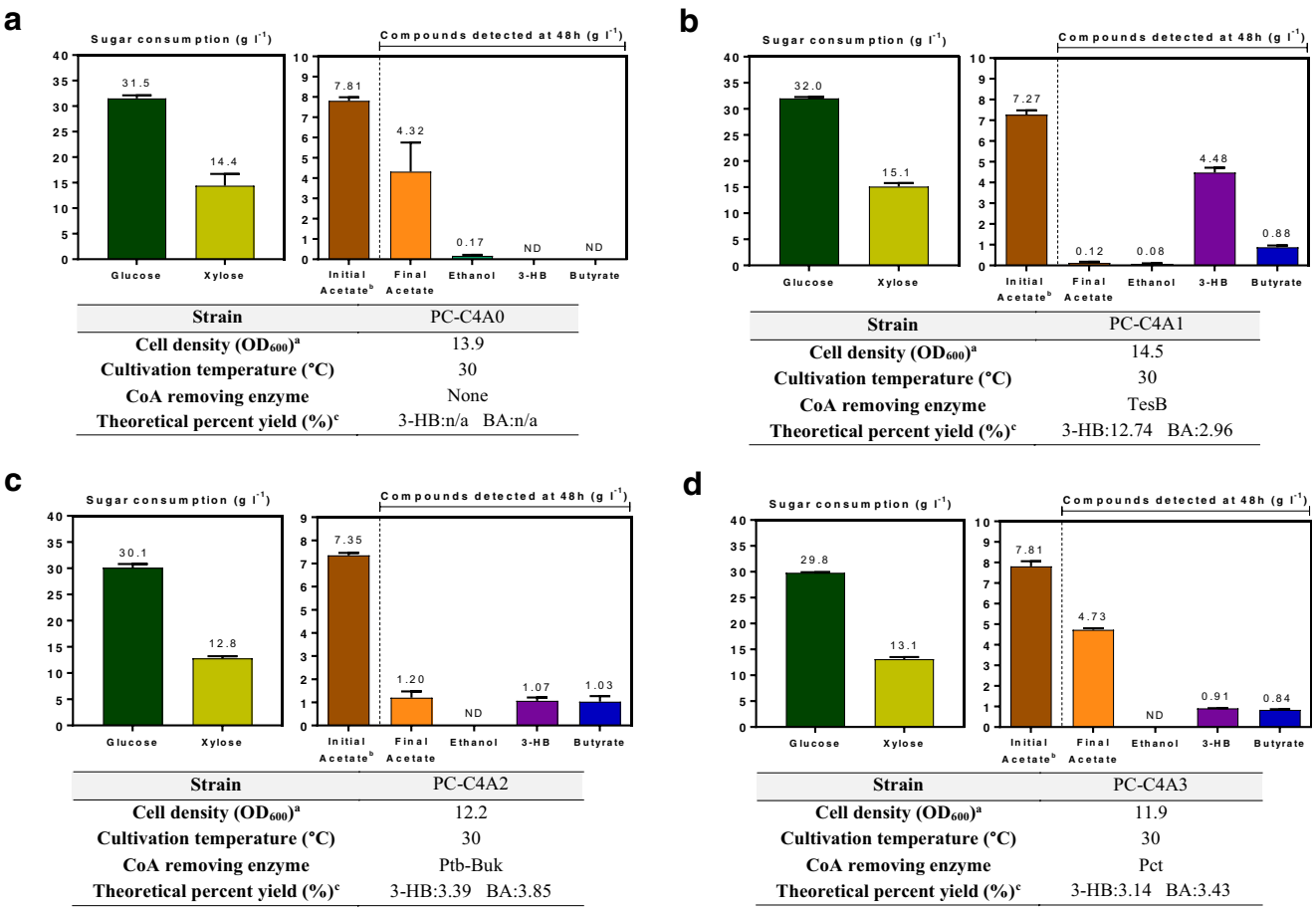

Strain	PC-C4A0
Cell density (OD_{600})[a]	13.9
Cultivation temperature (°C)	30
CoA removing enzyme	None
Theoretical percent yield (%)[c]	3-HB:n/a BA:n/a

Strain	PC-C4A1
Cell density (OD_{600})[a]	14.5
Cultivation temperature (°C)	30
CoA removing enzyme	TesB
Theoretical percent yield (%)[c]	3-HB:12.74 BA:2.96

Strain	PC-C4A2
Cell density (OD_{600})[a]	12.2
Cultivation temperature (°C)	30
CoA removing enzyme	Ptb-Buk
Theoretical percent yield (%)[c]	3-HB:3.39 BA:3.85

Strain	PC-C4A3
Cell density (OD_{600})[a]	11.9
Cultivation temperature (°C)	30
CoA removing enzyme	Pct
Theoretical percent yield (%)[c]	3-HB:3.14 BA:3.43

[a] Measured cell density after 48 h cultivation using spectrophotometer (OD_{600}), time 0 h cell density was kept at ~5.00
[b] Acetate concentration (g l^{-1}) at 0h
[c] Defined as the percentage of 3-HB/butyrate theoretical yields based on consumed glucose, xylose, and acetate
BA butyrate
n/a not applicable
ND not detected

Fig. 3 Evaluating CoA removal efficiency under 30 °C cultivation temperature. Sugar consumption, major metabolite titers, and final optical density during cultivation of PC-C4A0 (**a**), PC-C4A1 (**b**), PC-C4A2 (**c**), and PC-C4A3 (**d**). Error bars represent the mean ± SD (n = 3)

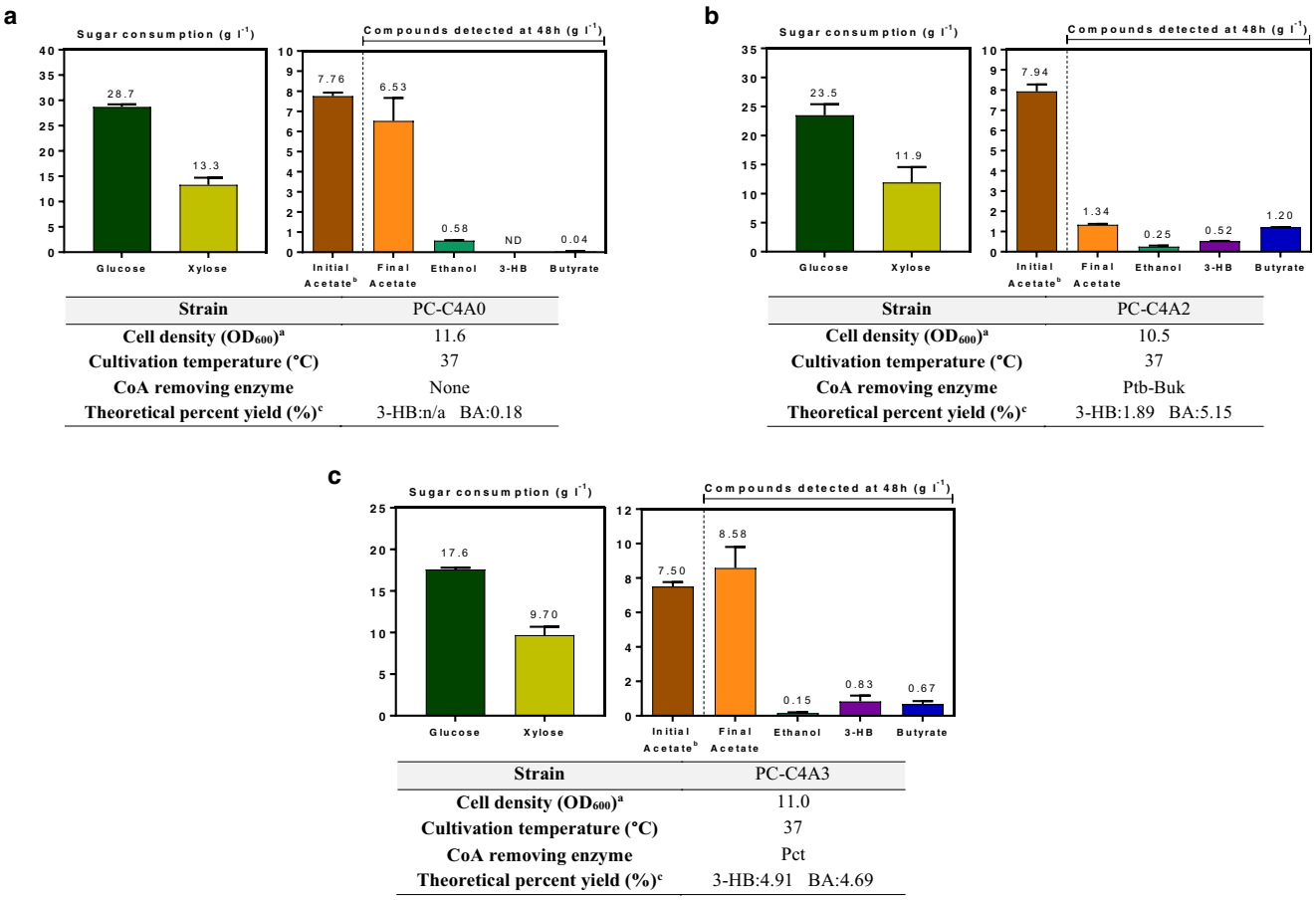

Strain	PC-C4A0
Cell density (OD_{600})[a]	11.6
Cultivation temperature (°C)	37
CoA removing enzyme	None
Theoretical percent yield (%)[c]	3-HB:n/a BA:0.18

Strain	PC-C4A2
Cell density (OD_{600})[a]	10.5
Cultivation temperature (°C)	37
CoA removing enzyme	Ptb-Buk
Theoretical percent yield (%)[c]	3-HB:1.89 BA:5.15

Strain	PC-C4A3
Cell density (OD_{600})[a]	11.0
Cultivation temperature (°C)	37
CoA removing enzyme	Pct
Theoretical percent yield (%)[c]	3-HB:4.91 BA:4.69

[a] Measured cell density after 48 h cultivation using spectrophotometer (OD_{600}), time 0 h cell density was kept at ~5.00
[b] Acetate concentration (g l^{-1}) at 0h
[c] Defined as the percentage of 3-HB/butyrate theoretical yields based on consumed glucose, xylose, and acetate
BA butyrate
n/a not applicable
ND not detected

Fig. 4 Evaluating CoA removal efficiency under 37 °C cultivation temperature. Sugar consumption, major metabolite titers, and final optical density during cultivation of PC-C4A0 (**a**), PC-C4A2 (**b**), and PC-C4A3 (**c**). Error bars represent the mean ± SD ($n = 3$)

fold that of the PhaB-PhaJ route in PC-BAR, implying that the Hbd-Crt route was more favorable than the PhaB-PhaJ route for the conversion from acetoacetyl-CoA to crotonyl-CoA. Note that the production of 3-HB was still observed in these engineered strains, i.e., 0.42 g L^{-1} and 0.02 g L^{-1} 3-HB for PC-BAR and PC-BAS, respectively. The significantly higher 3-HB titer for PC-BAR could imply a higher activity of Ptb-Buk toward (*R*)-3HB-CoA than (*S*)-3HB-CoA. Importantly, compared to PC-BAR and PC-BAS, the implementation of both RD routes in PC-BARS significantly improved butyrate production to 1.68 g L^{-1} (8.21% yield) with enhanced dissimilation of glucose, xylose, and acetate.

Manipulation of the 3-HB-producing pathway

To enhance the 3-HB production, we inactivated the competing pathways for butyrate formation without expressing the *crt*, *phaJ*, and *ter* genes. The production of (*R*)-3-HB and (*S*)-3-HB based on individual and both reduction routes via PhaB and/or Hbd in various engineered strains is summarized in Fig. 6. Note that TesB was used for CoA-removing enzyme as it previously showed the highest performance in the 3-HB production among the three CoA-removing enzymes evaluated. The biosynthesis of (*R*)-3-HB from PC-3HBR was approximately 1.6-fold that of (*S*)-3-HB from PC-3HBS. Importantly, coexpression of *phaB* and *hbd* in PC-3HBRS resulted in synergistic biosynthesis (*R*)/(S)-3-HB at 6.77 g L^{-1}, which is 1.4-fold that of the (*R*)/(S)-3-HB titer generated by 3-HB-butyrate-coproducing PC-C4A1. In addition, activating both PhaB and Hbd reductive routes in PC-3HBRS also significantly improved dissimilation of glucose, xylose, and acetate as well as cell growth. To further enhance the 3-HB production, we inactivated two global regulators, i.e., ArcA (encoded by *arcA*) and Fnr (encoded by *fnr*) in PC-3HBRS (Fig. 7). Both ArcA and Fnr have pleiotropic effects on various cellular functions (Kang et al. 2005; Kumar and

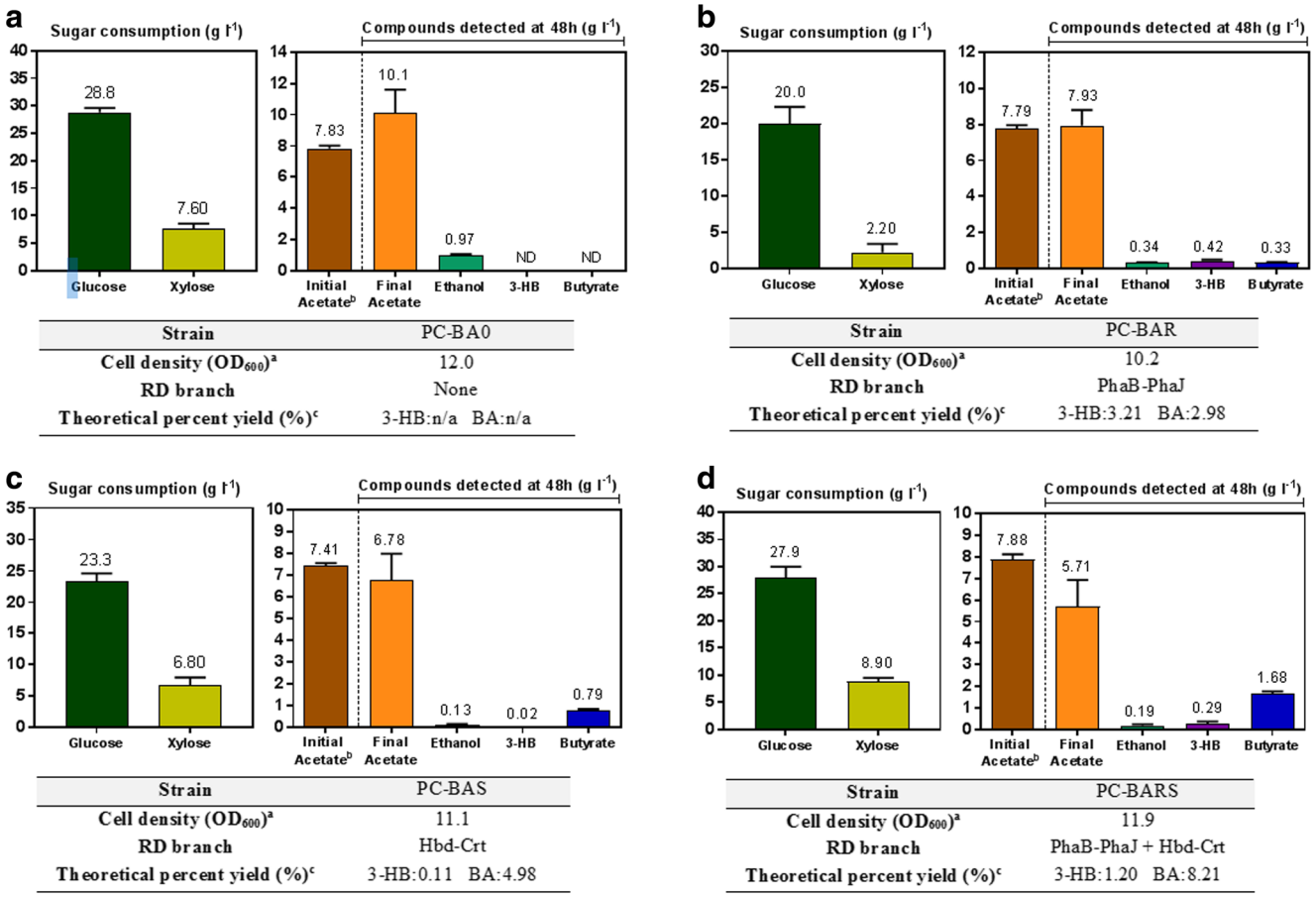

[a] Measured cell density after 48 h cultivation using spectrophotometer (OD_{600}), time 0 h cell density was kept at ~5.00
[b] Acetate concentration ($g l^{-1}$) at 0h
[c] Defined as the percentage of 3-HB/butyrate theoretical yields based on consumed glucose, xylose, and acetate
BA butyrate
n/a not applicable
ND not detected
RD reduction-dehydration

Fig. 5 Enhancing butyrate production by activating the second RD route. Sugar consumption, major metabolite titers, and final optical density during cultivation of PC-BA0 (**a**), PC-BAR (**b**), PC-BAS (**c**), and PC-BARS (**d**). Error bars represent the mean ± SD ($n = 3$)

Shimizu 2011; Park et al. 2013) and strict gene regulation under microaerobic and anaerobic conditions (Nikel et al. 2008b; Shalel Levanon et al. 2005). Strains carrying the *arcA* mutation have been reported to enhance PHB production under microaerobic conditions, presumably due to an increased reducing power caused by the activation of the TCA cycle (Nikel et al. 2010; Nikel et al. 2008a). On the other hand, the *fnr* mutant can downregulate *arcA* and decrease the flux through pyruvate formate-lyase (Pfl), potentially resulting in an intracellular accumulation of pyruvate (Marzan et al. 2011). Compared to the parental strain PC-3HBRS, the two regulator mutants, PC-3HBRSΔ*arcA* and PC-3HBRSΔ*fnr*, displayed an increase in the 3-HB production with the titers reaching 7.45 g L^{-1} (21.45% yield) and 8.95 g L^{-1} (25.33% yield), respectively. Note that PC-3HBRSΔ*fnr* had a statistically significant increase in the 3-HB production compared with PC-3HBRS. Moreover, carbon dissimilation in both mutants was extremely effective with almost no residual glucose, xylose, and acetate at the end of the cultivations.

Discussion

While major technological advances have been made in lignocellulose pretreatment, various inhibitory components from the lignocellulosic materials are released into the pretreating stream. The presence of these toxic compounds in the lignocellulose hydrolysate can limit the performance of microbial cultivation by inhibiting cell growth and carbon dissimilation, particularly for engineered bacterial strains which are often more sensitive to cultivation environment. In this study, we demonstrated effective microbial production of butyrate and 3-HB in engineered *E. coli* using $Ca(OH)_2$-detoxified lignocellulosic hydrolysate. In comparison to the defined medium,

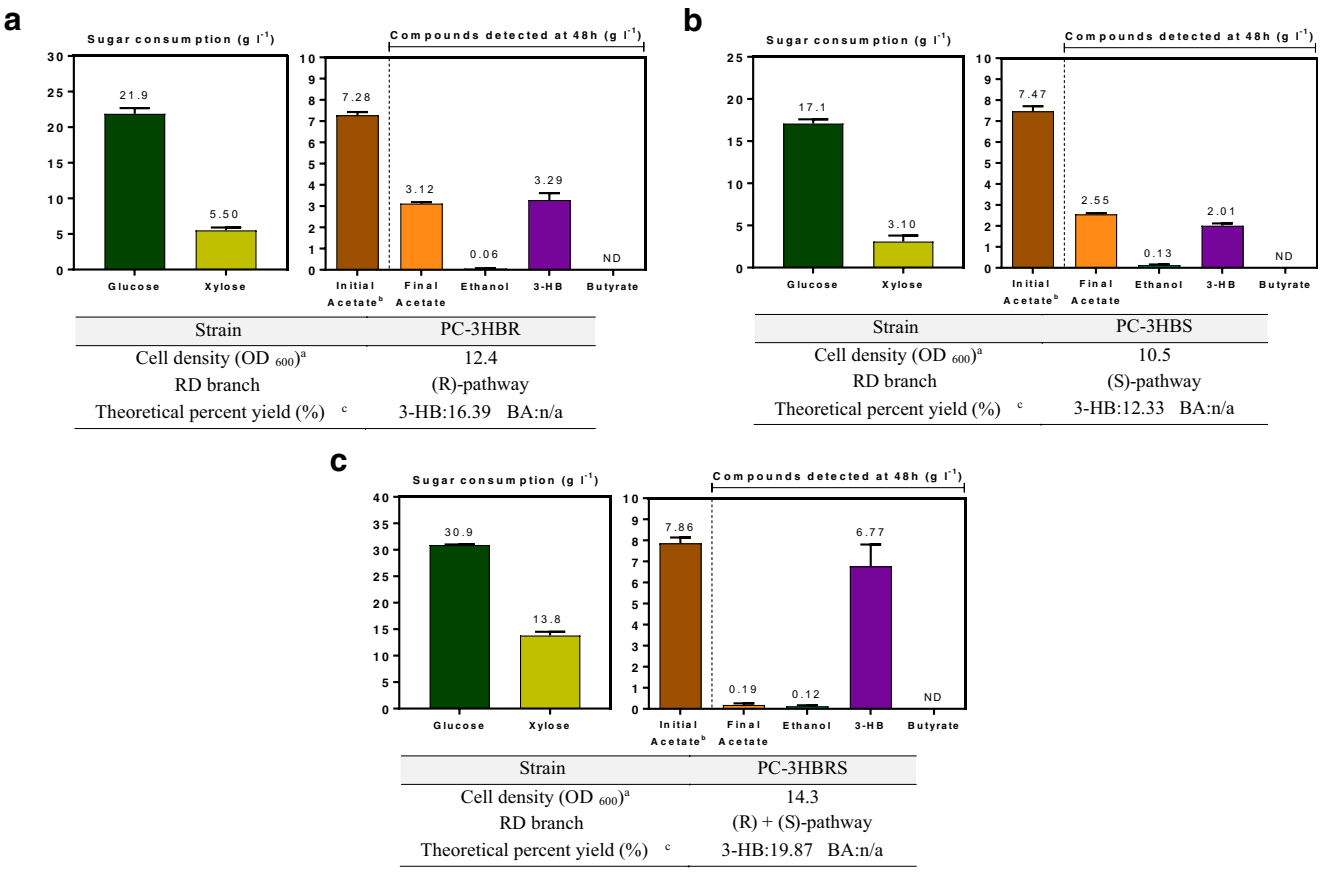

[a] Measured cell density after 48 h cultivation using spectrophotometer (OD_{600}), time 0 h cell density was kept at ~5.00
[b] Acetate concentration (g l^{-1}) at 0h
[c] Defined as the percentage of 3-HB/butyrate theoretical yields based on consumed glucose, xylose, and acetate
BA butyrate
n/a not applicable
ND not detected

Fig. 6 Biosynthesis of 3-HB by individual and combined *R*/*S* pathways. Sugar consumption, major metabolite titers, and final optical density during cultivation of PC-3HBR (**a**), PC-3HBS (**b**), and PC-3HBRS (**c**). Error bars represent the mean ± SD ($n = 3$)

using the original lignocellulosic hydrolysate for PC-C4A1 cultivation resulted in significant carbon diversion at the acetyl-CoA node from ethanol to acetate formation. Inhibition of alcohologenesis was previously observed in organisms exposed to furfural (Banerjee et al. 1981; Palmqvist et al. 1996), which is a common inhibitor found in untreated lignocellulosic hydrolysates (Heer and Sauer 2008; Kim et al. 2015; Li et al. 2015; Sárvári Horváth et al. 2003; Xiros and Olsson 2014). More specifically, furfural can directly bind and inactivate alcohol dehydrogenase (AdhE) in *E. coli* (Zaldivar et al. 1999). In addition to the carbon flux redirection at the acetyl-CoA node, the conserved reducing equivalents (i.e., NADH) caused by the limited ethanol production using the original hydrolysate may have led to a build-up of butyryl-CoA via NADH-dependent Ter, as evidenced by a higher butyrate titer in comparison to the culture using the defined medium.

Out of the two detoxification methods evaluated, $Ca(OH)_2$ treatment was more effective for the synthesis of 3-HB by PC-C4A1, albeit at the expense of a greater sugar loss compared with NH_4OH treatment. Interestingly, $Ca(OH)_2$ treatment significantly increased the dissimilation rate of glucose and xylose by 1.7-fold and 3.1-fold, respectively. More importantly, the $Ca(OH)_2$ treatment could also indirectly result in effective acetate dissimilation, almost depleting acetate in the original hydrolysate. Such a carbon dissimulation pattern can be associated with carbon catabolite repression as acetate is the next preferred carbon source after exhaustion of glucose and xylose. Since acetate is a related carbon source to form acetyl-CoA as a precursor to 3-HB, its elevated dissimilation may be a contributing factor to the enhanced 3-HB production. Previously, it was reported that $Ca(OH)_2$ treatment can enhance sugar utilization as a result of the elimination of lignin-derived inhibitors (Amartey and Jeffries 1996), presumably due to the binding and precipitation of these toxic chemicals with the Ca^{2+} ion (Van Zyl et al. 1988). The efficient removal of lignin-derived inhibitors for the $Ca(OH)_2$ treatment could mediate the enhanced carbon dissimilation

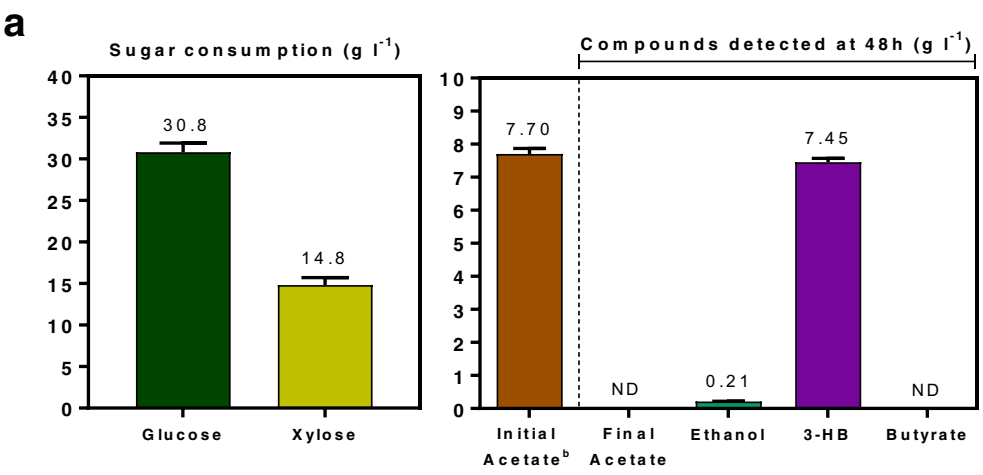

Strain	PC-3HBRSΔ *arcA*
Cell density (OD_{600})[a]	14.6
Inactivated regulator	ArcA
Theoretical percent yield (%)[c]	3-HB:21.45 BA:n/a

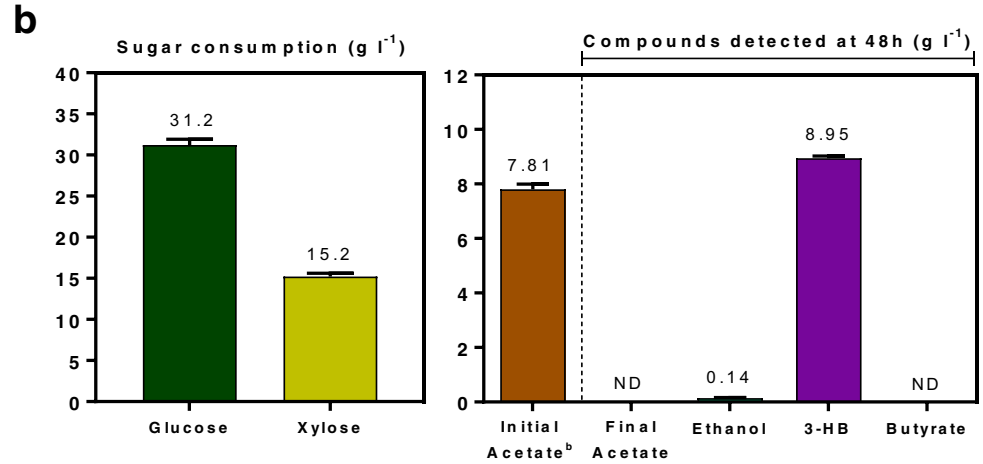

Strain	PC-3HBRSΔ *fnr*
Cell density (OD_{600})[a]	14.9
Inactivated regulator	Fnr
Theoretical percent yield (%)[c]	3-HB:25.33 BA:n/a

Fig. 7 Improving biosynthesis of 3-HB by inactivating key aeration regulators. Sugar consumption, major metabolite titers, and final optical density during cultivation of PC-3HBRSΔ*arcA* (**a**) and PC-3HBRSΔ*fnr* (**b**). Error bars represent the mean ± SD (n = 3)

and conversion to 3-HB in PC-C4A1. Despite the reported enhanced microbial fermentability for the hydrolysate treated with NH_4OH (Alriksson et al. 2005a; Alriksson et al. 2006; Persson et al. 2002a), our results showed no positive effects for the NH_4OH treatment. It has been reported that an accumulation of unknown precipitate may occur as a result of aldol condensation of furan aldehydes and ammonia (Alriksson et al. 2006), potentially interfering with metabolic activity of *E. coli*.

Among a selection of engineered *E. coli* strains harboring different CoA-removing genes (i.e., *tesB*, *ptb-buk*, and *pct*) evaluated for the coproduction of butyrate and 3-HB using the $Ca(OH)_2$-treated hydrolysate, PC-C4A1 and PC-C4A2 demonstrated the highest 3-HB and butyrate production, respectively, at 37 °C. The native TesB was the most effective CoA-removing enzyme for 3-HB production potentially due to its wide-range substrate specificity (Tseng et al. 2009). In addition, TesB has been reported to prevent an abnormal accumulation of intracellular acyl-CoA moieties in *E. coli* (Zheng et al. 2004), and such metabolic capacity can potentially drive effective utilization of intracellular acetyl-CoA, as observed by the enhanced dissimilation of various carbons

including acetate for PC-C4A1. On the other hand, Ptb-Buk expressed in PC-C4A2 mediated the highest conversion of butyryl-CoA to butyrate in comparison to TesB and Pct. Note that Ptb-Buk can have a high enzyme specificity toward butyryl-CoA as it originates from a natural butyrate-producing organism (Holt et al. 1984; Jang et al. 2013).

The reduction-dehydration (RD) routes contain the Hbd-Crt and PhaB-PhaJ pathways in parallel for the biosynthesis of 1-butanol and butyrate via (*S*)- and (*R*)-3-HB-CoA, respectively (Fig. 1), in various host organisms (Choi et al. 2014; Lamsen and Atsumi 2012; Lan and Liao 2012). Using the $Ca(OH)_2$-treated hydrolysate for the cultivation of PC-BAS and PC-BAR (for both of which Ptb-Buk was used as a CoA-removing enzyme), it appears that butyrate production was favored by the Hbd-Crt pathway in comparison to the PhaB-PhaJ pathway. Note that Ptb-Buk has a very low affinity toward (*S*)-3-HB-CoA and does not generally produce (*S*)-3-HB in high amounts (Tseng et al. 2009). This is consistent with our current results as PC-BAS hardly produced (*S*)-3-HB and the dissimilated carbon flux was primarily directed toward butyrate production. On the other hand, Ptb-Buk may cause significant carbon diversion at the (*R*)-3-HB-CoA node toward (*R*)-3-HB in PC-BAR and reduced butyrate production as a result. Furthermore, butyrate production was synergistically enhanced with more effective carbon dissimilation upon coexpression of Hbd-Crt and PhaB-PhaJ, suggesting more balanced carbon flux through the butyrate-formation pathways when the two RD routes were activated. Given that both reduction steps are NADH-dependent, the rather low butyrate yield can be potentially enhanced by genetic elimination of competing NADH-consuming pathways to conserve reducing equivalents and drive carbon flux through the RD route (Baek et al. 2013).

To enhance the 3-HB production using the $Ca(OH)_2$-treated hydrolysate, we derived strains with no butyrate-producing pathway and also evaluated the contribution of individual *R*/*S* pathways for the 3-HB formation. PC-3HBR produced significantly more 3-HB than PC-3HBS, suggesting that the *R*-pathway was more favored than the *S*-pathway for 3-HB formation. The intracellular levels of reducing equivalents of NADH and NADPH can alter the catalytic activities of Hbd and PhaB, respectively, yielding different levels of (*S*)-3-HB and (*R*)-3HB. Moreover, it has been reported that the physiological ratios of $NADH/NAD^+$ and $NADPH/NADP^+$, rather than the NADH/NADPH ratio, influence the distributive production of (*S*)/(*R*)-3-HB (Tseng et al. 2009). Also, PHB production appears to be more related to the $NADPH/NADP^+$ ratio (Lee et al. 1996), further supporting the argument of the dominant *R*-pathway for 3-HB production. Coexpression of the *R*- and *S*-pathways in PC-3HBRS enhanced cell growth and carbon dissimilation with significantly increased 3-HB production, implying that both the intracellular NADH and NADPH levels could be properly regulated for driving effective 3-HB conversion.

The metabolic profile of *E. coli* upon carbon dissimilation is highly influenced by the availability of oxygen (Alexeeva et al. 2002; Shalel-Levanon et al. 2005; Shalel Levanon et al. 2005). Basically, pyruvate, the final product of glycolysis, is oxidized via the TCA cycle with the formation of reducing equivalents under aerobic conditions, or is catabolized via various fermentative pathways under anaerobic conditions (Shalel Levanon et al. 2005). The metabolic switch is mediated by protein regulators, such as ArcA and Fnr, in response to the changing levels of oxygen or other electron acceptors (Gunsalus 1992). ArcA is upregulated under the initial onset of anaerobiosis, whereas Fnr is upregulated if the oxygen limitation persists (Förster and Gescher 2014; Sawers and Suppmann 1992). As the expression of these regulators can impact cell physiology and biotransformation, they often become targets for genetic manipulation. For example, mutation of *arcA* or *fnr* was effective to enhance PHB production in *E. coli* (Nikel et al. 2006; Nikel et al. 2008a) potentially due to the relaxed repression of the TCA cycle genes and the conserved reducing equivalents (Alexeeva et al. 2002; Nikel et al. 2006). Similar genetic effects associated with *arcA* or *fnr* inactivation have been reported to increase the production of other chemicals in *E. coli*, such as 1,4-butanediol (Yim et al. 2011), lactate (Shalel Levanon et al. 2005), and 1,3-propanediol (Egoburo et al. 2018). In this study, compared to the parental strain PC-3HBRS, 3-HB biosynthesis was improved by inactivating *arcA* and *fnr* in PC-3HBRSΔ*arcA* and PC-3HBRSΔ*fnr*, respectively. Note that carbon dissimilation was rather complete, even for acetate, in both mutant strains, suggesting not only a balanced formation of reducing equivalents of NADH and NADPH but also the abundance of the acetyl-CoA precursor for enhanced 3-HB production. To further enhance 3-HB production, inactivation of other global regulators, such as Cra encoded by *cra*, could be explored as mutation in *cra* has previously been reported to improve both cell growth and glucose consumption compared to *arcA* and *fnr* mutations in *E. coli* (Perrenoud and Sauer 2005). Hence, the inactivation of global regulators exemplifies an exceptional genetic strategy toward 3-HB production from cheap lignocellulosic feedstock.

Acknowledgment The authors' research is supported by Natural Sciences and Engineering Research Council (NSERC) and Networks of Centres of Excellence of Canada (BioFuelNet).

Compliance with ethical standards

Conflict of interest The authors declare that they have no competing interests.

Ethical approval This article does not contain any studies with human participants or animals performed by any of the authors.

References

Achinas S, Euverink GJW. (2016). Consolidated briefing of biochemical ethanol production from lignocellulosic biomass. EJB 23(Supplement C):44–53

Akawi L, Srirangan K, Liu X, Moo-Young M, Perry CC (2015) Engineering *Escherichia coli* for high-level production of propionate. J Ind Microbiol Biotechnol 42(7):1057–1072

Alexeeva S, Hellingwerf KJ, Teixeira de Mattos MJ (2002) Quantitative assessment of oxygen availability: perceived aerobiosis and its effect on flux distribution in the respiratory chain of *Escherichia coli*. J Bacteriol 184(5):1402–1406

Alriksson B, Horvath IS, Sjöde A, Nilvebrant N-O, Jönsson LJ (2005a) Ammonium hydroxide detoxification of spruce acid hydrolysates. In: Davison BH, Evans BR, Finkelstein M, McMillan JD (eds) Twenty-sixth symposium on biotechnology for fuels and chemicals. Humana Press, Totowa, pp 911–922

Alriksson B, Horváth IS, Sjöde A, Nilvebrant N-O, Jönsson LJ (2005b) Ammonium hydroxide detoxification of spruce acid hydrolysates. Appl Biochem Biotechnol 124(1):911–922

Alriksson B, Sjöde A, Nilvebrant N-O, Jönsson LJ (2006) Optimal conditions for alkaline detoxification of dilute-acid lignocellulose hydrolysates. Appl Biochem Biotechnol 130(1):599–611

Alriksson B, Cavka A, Jönsson LJ (2011) Improving the fermentability of enzymatic hydrolysates of lignocellulose through chemical in-situ detoxification with reducing agents. Bioresour Technol 102(2): 1254–1263

Amann E, Ochs B, Abel K-J (1988) Tightly regulated tac promoter vectors useful for the expression of unfused and fused proteins in *Escherichia coli*. Gene 69(2):301–315

Amartey S, Jeffries T (1996) An improvement in *Pichia stipitis* fermentation of acid-hydrolysed hemicellulose achieved by overliming (calcium hydroxide treatment) and strain adaptation. World J Microbiol Biotechnol 12(3):281–283

Baba T, Ara T, Hasegawa M, Takai Y, Okumura Y, Baba M, Datsenko KA, Tomita M, Wanner BL, Mori H (2006) Construction of *Escherichia coli* K-12 in-frame, single-gene knockout mutants: the Keio collection. Mol Syst Biol 2

Baek J-M, Mazumdar S, Lee S-W, Jung M-Y, Lim J-H, Seo S-W, Jung G-Y, Oh M-K (2013) Butyrate production in engineered *Escherichia coli* with synthetic scaffolds. Biotechnol Bioeng 110(10):2790–2794

Balan V (2014) Current challenges in commercially producing biofuels from lignocellulosic biomass. ISRN Biotechnology 2014:31

Banerjee N, Bhatnagar R, Viswanathan L (1981) Inhibition of glycolysis by furfural in *Saccharomyces cerevisiae*. Euro J Appl Microbiol Biotechnol 11(4):226–228

Bond-Watts BB, Bellerose RJ, Chang MCY (2011) Enzyme mechanism as a kinetic control element for designing synthetic biofuel pathways. Nat Chem Biol 7:222–227

Brodeur G, Yau E, Badal K, Collier J, Ramachandran KB, Ramakrishnan S (2011) Chemical and physicochemical pretreatment of lignocellulosic biomass: a review. J Enzym Res 2011:17

Carriquiry MA, Du X, Timilsina GR (2011) Second generation biofuels: economics and policies. Energy Policy 39(7):4222–4234

Cavka A, Jönsson LJ. 2013. Detoxification of lignocellulosic hydrolysates using sodium borohydride. Bioresour Technol 136 (Supplement C):368–376

Cherepanov PP, Wackernagel W (1995) Gene disruption in *Escherichia coli*: TcR and KmR cassettes with the option of Flp-catalyzed excision of the antibiotic-resistance determinant. Gene 158(1):9–14

Choi YJ, Lee J, Jang Y-S, Lee SY (2014) Metabolic engineering of microorganisms for the production of higher alcohols. mBio 5(5): e01524-14

Coz A, Llano T, Cifrián E, Viguri J, Maican E, Sixta H (2016) Physicochemical alternatives in lignocellulosic materials in relation to the kind of component for fermenting purposes. Materials 9(7):574

Datsenko KA, Wanner BL (2000) One-step inactivation of chromosomal genes in *Escherichia coli* K-12 using PCR products. Proc Natl Acad Sci 97(12):6640–6645

Delidovich I, Hausoul PJC, Deng L, Pfützenreuter R, Rose M, Palkovits R (2016) Alternative monomers based on lignocellulose and their use for polymer production. Chem Rev 116(3):1540–1599

Dionisi D, Anderson JA, Aulenta F, McCue A, Paton G (2015) The potential of microbial processes for lignocellulosic biomass conversion to ethanol: a review. J Chem Technol Biotechnol 90(3):366–383

Dwidar M, Park J-Y, Mitchell RJ, Sang B-I (2012) The future of butyric acid in industry. Sci World J 2012:471417

Egoburo DE, Diaz Peña R, Alvarez DS, Godoy MS, Mezzina MP, Pettinari MJ (2018) Microbial cell factories à la carte: elimination of global regulators Cra and ArcA generates metabolic backgrounds suitable for the synthesis of bioproducts in *Escherichia coli*. Appl Environ Microbiol 84

El-Shahawy Tarek Abd E-G. (2015) Chemicals with a natural reference for controlling water hyacinth, *Eichhornia crassipes* (Mart.) Solms. J Plant Protect Res. p 294

Entin-Meer M, Rephaeli A, Yang X, Nudelman A, VandenBerg SR, Haas-Kogan DA (2005) Butyric acid prodrugs are histone deacetylase inhibitors that show antineoplastic activity and radiosensitizing capacity in the treatment of malignant gliomas. Mol Cancer Ther 4(12):1952–1961

Fakhrudin J, Setyaningsih D, Rahayuningsih M (2014) Bioethanol production from seaweed *Eucheuma cottonii* by neutralization and detoxification of acidic catalyzed hydrolysate. 455–458 p.

Fenske JJ, Griffin DA, Penner MH (1998) Comparison of aromatic monomers in lignocellulosic biomass prehydrolysates. J Ind Microbiol Biotechnol 20(6):364–368

Förster AH, Gescher J (2014) Metabolic engineering of *Escherichia coli* for production of mixed-acid fermentation end products. Front Bioeng Biotechnol 2(16)

Gibson DG, Young L, Chuang R-Y, Venter JC, Hutchison CA, Smith HO (2009) Enzymatic assembly of DNA molecules up to several hundred kilobases. Nat Meth 6(5):343–345

Guevara-Martínez M, Gällnö KS, Sjöberg G, Jarmander J, Perez-Zabaleta M, Quillaguamán J, Larsson G (2015) Regulating the production of (*R*)-3-hydroxybutyrate in *Escherichia coli* by N or P limitation. Front Microbiol 6(AUG):844

Gulevich AY, Skorokhodova AY, Sukhozhenko AV, Debabov VG (2017) Biosynthesis of enantiopure (*S*)-3-hydroxybutyrate from glucose through the inverted fatty acid β-oxidation pathway by metabolically engineered *Escherichia coli*. J Biotechnol 244(Supplement C): 16–24

Gunsalus RP (1992) Control of electron flow in *Escherichia coli*: coordinated transcription of respiratory pathway genes. J Bacteriol 174(22):7069–7074

Heer D, Sauer U (2008) Identification of furfural as a key toxin in lignocellulosic hydrolysates and evolution of a tolerant yeast strain. Microbial Biotechnol 1(6):497–506

Holt RA, Stephens GM, Morris JG (1984) Production of solvents by *Clostridium acetobutylicum* cultures maintained at neutral pH. Appl Environ Microbiol 48(6):1166–1170

Jang Y-S, Woo HM, Im JA, Kim IH, Lee SY (2013) Metabolic engineering of *Clostridium acetobutylicum* for enhanced production of butyric acid. Appl Microbiol Biotechnol 97(21):9355–9363

Jarmander J, Belotserkovsky J, Sjöberg G, Guevara-Martínez M, Pérez-Zabaleta M, Quillaguamán J, Larsson G (2015) Cultivation strategies for production of (*R*)-3-hydroxybutyric acid from simultaneous consumption of glucose, xylose and arabinose by *Escherichia coli*. Microb Cell Factories 14(1):51

Jawed K, Mattam AJ, Fatma Z, Wajid S, Abdin MZ, Yazdani SS (2016) Engineered production of short chain fatty acid in *Escherichia coli* using fatty acid synthesis pathway. PLoS One 11(7):e0160035

Jha AK, Li J, Yuan Y, Baral N, Ai B (2014) A review on bio-butyric acid production and its optimization. 1019–1024 p.

Jiang Y, Zeng X, Luque R, Tang X, Sun Y, Lei T, Liu S, Lin L (2017) Cooking with active oxygen and solid alkali: a promising alternative approach for lignocellulosic biorefineries. ChemSusChem 10(20): 3982–3993

Jobling MG, Holmes RK (1990) Construction of vectors with the p15a replicon, kanamycin resistance, inducible lacZ alpha and pUC18 or pUC19 multiple cloning sites. Nucleic Acids Res 18(17):5315–5316

Jönsson LJ, Palmqvist E, Nilvebrant N-O, Hahn-Hägerdal B (1998) Detoxification of wood hydrolysates with laccase and peroxidase from the white-rot fungus *Trametes versicolor*. Appl Microbiol Biotechnol 49(6):691–697

Jönsson LJ, Alriksson B, Nilvebrant N-O (2013) Bioconversion of lignocellulose: inhibitors and detoxification. Biotechnology for Biofuels 6:6–16

Kang Y, Weber KD, Qiu Y, Kiley PJ, Blattner FR (2005) Genome-wide expression analysis indicates that FNR of *Escherichia coli* K-12 regulates a large number of genes of unknown function. J Bacteriol 187(3):1135–1160

Kim SB, Lee JH, Yang X, Lee J, Kim SW (2015) Furfural production from hydrolysate of barley straw after dilute sulfuric acid pretreatment. Korean J Chem Eng 32(11):2280–2284

Kumar R, Shimizu K (2011) Transcriptional regulation of main metabolic pathways of cyoA, cydB, fnr, and fur gene knockout *Escherichia coli* in C-limited and N-limited aerobic continuous cultures. Microb Cell Factories 10:3–3

Lamsen EN, Atsumi S (2012) Recent progress in synthetic biology for microbial production of C3–C10 alcohols. Front Microbiol 3:196

Lan EI, Liao JC (2012) ATP drives direct photosynthetic production of 1-butanol in cyanobacteria. Proc Natl Acad Sci 109(16):6018–6023

Larsson S, Reimann A, Nilvebrant N-O, Jönsson LJ (1999) Comparison of different methods for the detoxification of lignocellulose hydrolyzates of spruce. Appl Biochem Biotechnol 77(1):91–103

Lee IY, Kim MK, Park YH, Lee SY (1996) Regulatory effects of cellular nicotinamide nucleotides and enzyme activities on poly (3-hydroxybutyrate) synthesis in recombinant *Escherichia coli*. Biotechnol Bioeng 52(6):707–712

Li H, Chen X, Ren J, Deng H, Peng F, Sun R (2015) Functional relationship of furfural yields and the hemicellulose-derived sugars in the hydrolysates from corncob by microwave-assisted hydrothermal pretreatment. Biotechnol Biofuels 8:127

López MJ, Nichols NN, Dien BS, Moreno J, Bothast RJ (2004) Isolation of microorganisms for biological detoxification of lignocellulosic hydrolysates. Appl Microbiol Biotechnol 64(1):125–131

Martinez A, Rodriguez M, York S, Preston J, Ingram L (2000) Effect of Ca(OH)2 treatments on the composition and toxicity of bagasse hemicellulose hydrolysates. 526–536 p.

Martinez A, Rodriguez ME, Wells ML, York SW, Preston JF, Ingram LO (2001) Detoxification of dilute acid hydrolysates of lignocellulose with lime. Biotechnol Prog 17(2):287–293

Marzan LW, Siddiquee KAZ, Shimizu K (2011) Metabolic regulation of an fnr gene knockout *Escherichia coli* under oxygen limitation. Bioeng Bugs 2(6):331–337

Miller JH (1992) A short course in bacterial genetics: a laboratory manual and handbook for *Escherichia coli* and related bacteria. Cold Spring Harbor Laboratory Press, NY

Mohr A, Raman S (2013) Lessons from first generation biofuels and implications for the sustainability appraisal of second generation biofuels. Energy Policy 63(Supplement C):114–122.

Nikel PI, Pettinari MJ, Galvagno MA, Méndez BS (2006) Poly(3-hydroxybutyrate) synthesis by recombinant *Escherichia coli* arcA mutants in microaerobiosis. Appl Microbiol Biotechnol 72(4): 2614–2620

Nikel PI, Pettinari MJ, Galvagno MA, Méndez BS (2008a) Poly(3-hydroxybutyrate) synthesis from glycerol by a recombinant *Escherichia coli* arcA mutant in fed-batch microaerobic cultures. Appl Microbiol Biotechnol 77(6):1337–1343

Nikel PI, Pettinari MJ, Ramírez MC, Galvagno MA, Méndez BS (2008b) *Escherichia coli arcA* mutants: metabolic profile characterization of microaerobic cultures using glycerol as a carbon source. J Mol Microbiol Biotechnol 15(1):48–54

Nikel PI, de Almeida A, Giordano AM, Pettinari MJ (2010) Redox driven metabolic tuning. Bioeng Bugs 1(4):293–297

Okuda N, Soneura M, Ninomiya K, Katakura Y, Shioya S (2008) Biological detoxification of waste house wood hydrolysate using *Ureibacillus thermosphaericus* for bioethanol production. J Biosci Bioeng 106(2):128–133

Palmqvist E, Hahn-Hägerdal B, Galbe M, Zacchi G (1996) The effect of water-soluble inhibitors from steam-pretreated willow on enzymatic hydrolysis and ethanol fermentation. Enzym Microb Technol 19(6): 470–476

Panagiotopoulos IA, Chandra RP, Saddler JN (2013) A two-stage pretreatment approach to maximise sugar yield and enhance reactive lignin recovery from poplar wood chips. Bioresour Technol 130: 570–577

Park DM, Akhtar MS, Ansari AZ, Landick R, Kiley PJ (2013) The bacterial response regulator ArcA uses a diverse binding site architecture to regulate carbon oxidation globally. PLoS Genet 9(10): e1003839

Perez-Zabaleta M, Sjöberg G, Guevara-Martínez M, Jarmander J, Gustavsson M, Quillaguamán J, Larsson G (2016) Increasing the production of (*R*)-3-hydroxybutyrate in recombinant *Escherichia coli* by improved cofactor supply. Microb Cell Factories 15:91

Perrenoud A, Sauer U (2005) Impact of global transcriptional regulation by ArcA, ArcB, Cra, Crp, Cya, Fnr, and Mlc on glucose catabolism in *Escherichia coli*. J Bacteriol 187(9):3171–3179

Persson P, Andersson J, Gorton L, Larsson S, Nilvebrant N-O, Jönsson LJ (2002a) Effect of different forms of alkali treatment on specific fermentation inhibitors and on the fermentability of lignocellulose hydrolysates for production of fuel ethanol. J Agric Food Chem 50(19):5318–5325

Persson P, Larsson S, Jönsson LJ, Nilvebrant N-O, Sivik B, Munteanu F, Thörneby L, Gorton L (2002b) Supercritical fluid extraction of a lignocellulosic hydrolysate of spruce for detoxification and to facilitate analysis of inhibitors. Biotechnol Bioeng 79(6):694–700

Ranatunga TD, Jervis J, Helm RF, McMillan JD, Wooley RJ (2000) The effect of overliming on the toxicity of dilute acid pretreated lignocellulosics: the role of inorganics, uronic acids and ether-soluble organics. Enzym Microb Technol 27(3):240–247

Ren Q, Ruth K, Thöny-Meyer L, Zinn M (2010) Enatiomerically pure hydroxycarboxylic acids: current approaches and future perspectives. Appl Microbiol Biotechnol 87(1):41–52

Saini JK, Saini R, Tewari L (2015) Lignocellulosic agriculture wastes as biomass feedstocks for second-generation bioethanol production: concepts and recent developments. 3. Biotech 5(4):337–353

Sárvári Horváth I, Franzén CJ, Taherzadeh MJ, Niklasson C, Lidén G (2003) Effects of furfural on the respiratory metabolism of *Saccharomyces cerevisiae* in glucose-limited chemostats. Appl Environ Microbiol 69(7):4076–4086

Sateesh LR, Adivikatla V, Naseeruddin S, Yadav DS, Panda SH, Yenumula GP, Linga V (2011) Studies on different detoxification methods for the acid hydrolysate of lignocellulosic substrate *Saccharum spontaneum*. 53–57 p.

Sawers G, Suppmann B (1992) Anaerobic induction of pyruvate formate-lyase gene expression is mediated by the ArcA and FNR proteins. J Bacteriol 174(11):3474–3478

Shalel Levanon S, San K-Y, Bennett GN (2005) Effect of oxygen on the *Escherichia coli* ArcA and FNR regulation systems and metabolic responses. Biotechnol Bioeng 89(5):556–564

Shalel-Levanon S, San K-Y, Bennett GN (2005) Effect of ArcA and FNR on the expression of genes related to the oxygen regulation and the glycolysis pathway in *Escherichia coli* under microaerobic growth conditions. Biotechnol Bioeng 92(2):147–159

Tian D, Chandra RP, Lee J-S, Lu C, Saddler JN (2017) A comparison of various lignin-extraction methods to enhance the accessibility and ease of enzymatic hydrolysis of the cellulosic component of steam-pretreated poplar. Biotechnol Biofuels 10(1):157

Tokiwa Y, Ugwu CU (2007) Biotechnological production of (*R*)-3-hydroxybutyric acid monomer. J Biotechnol 132(3):264–272

Tseng H-C, Martin CH, Nielsen DR, Prather KLJ (2009) Metabolic engineering of *Escherichia coli* for enhanced production of (*R*)- and (*S*)-3-hydroxybutyrate. Appl Environ Microbiol 75(10):3137–3145

Ulbricht RJ, Northup SJ, Thomas JA (1984) A review of 5-hydroxymethylfurfural (HMF) in parenteral solutions. Fundam Appl Toxicol 4(5):843–53

Valdivia M, Galan JL, Laffarga J, Ramos J-L (2016) Biofuels 2020: biorefineries based on lignocellulosic materials. Microb Biotechnol 9(5):585–594

Valentine J, Clifton-Brown J, Hastings A, Robson P, Allison G, Smith P (2012) Food vs. fuel: the use of land for lignocellulosic 'next generation' energy crops that minimize competition with primary food production. GCB Bioenergy 4(1):1–19

Van Zyl C, Prior BA, Du Preez JC (1988) Production of ethanol from sugar cane bagasse hemicellulose hydrolyzate by *Pichia stipitis*. Appl Biochem Biotechnol 17(1):357–369

Volker AR, Gogerty DS, Bartholomay C, Hennen-Bierwagen T, Zhu H, Bobik TA (2014) Fermentative production of short-chain fatty acids in *Escherichia coli*. Microbiology 160(Pt_7):1513–1522

Welton T (2015) Solvents and sustainable chemistry. Proc Math Phys Eng Sci 471(2183):20150502

Wood BJB (1998) Microbiology of fermented foods. Springer, New York

Xiros C, Olsson L (2014) Comparison of strategies to overcome the inhibitory effects in high-gravity fermentation of lignocellulosic hydrolysates. Biomass Bioenergy 65 (Supplement C):79–90

Yim H, Haselbeck R, Niu W, Pujol-Baxley C, Burgard A, Boldt J, Khandurina J, Trawick JD, Osterhout RE, Stephen R and others. 2011. Metabolic engineering of *Escherichia coli* for direct production of 1,4-butanediol. Nat Chem Biol 7:445, 452

Yu RJ, Van Scott EJ (2004) Alpha-hydroxyacids and carboxylic acids. J Cosmet Dermatol 3(2):76–87

Zaldivar J, Martinez A, Ingram L (1999) Effect of selected aldehydes on the growth and fermentation of ethanologenic *Escherichia coli*. 24–33 p.

Zheng Z, Gong Q, Liu T, Deng Y, Chen J-C, Chen G-Q (2004) Thioesterase II of *Escherichia coli* plays an important role in 3-hydroxydecanoic acid production. Appl Environ Microbiol 70(7): 3807–3813